molecular pharmaceutics

Article

pubs.acs.org/molecularpharmaceutics

Curcumin-Loaded Blood-Stable Polymeric Micelles for Enhancing Therapeutic Effect on Erythroleukemia

Feirong Gong,[†,⊥] Dan Chen,[§,⊥] Xin Teng,[†] Junhua Ge,[∥] Xianfeng Ning,[∥] Ya-ling Shen,[§] Jian Li,[*,∥] and Shanfeng Wang[*,‡]

[†]Key Laboratory for Ultrafine Materials of Ministry of Education, School of Materials Science and Engineering, East China University of Science and Technology, Shanghai 200237, China

[§]State Key Laboratory of Bioreactor Engineering, Shanghai Collaborative Innovation Center for Biomanufacturing Technology, School of Biotechnology, East China University of Science and Technology, Shanghai 200237, China

[∥]Department of Cardiology, The Affiliated Hospital of Qingdao University, Qingdao 266003, China

[‡]Department of Materials Science and Engineering, The University of Tennessee, Knoxville, Tennessee 37996, United States

Supporting Information

ABSTRACT: Curcumin has high potential in suppressing many types of cancer and overcoming multidrug resistance in a multifaceted manner by targeting diverse molecular targets. However, the rather low systemic bioavailability resulted from its poor solubility in water and fast metabolism/excretion *in vivo* has hampered its applications in cancer therapy. To increase the aqueous solubility of curcumin while retaining the stability in blood circulation, here we report curcumin-loaded copolymer micelles with excellent *in vitro* and *in vivo* stability and antitumor efficacy. The two copolymers used for comparison were methoxy-poly(ethylene glycol)-*block*-poly(ε-caprolactone) (mPEG−PCL) and *N*-(*tert*-butoxycarbonyl)-L-phenylalanine end-capped mPEG−PCL (mPEG−PCL−Phe(Boc)). *In vitro* cytotoxicity evaluation against human pancreatic SW1990 cell line showed that the delivery of curcumin in mPEG−PCL−Phe(Boc) micelles to cancer cells was efficient and dosage-dependent. The pharmacokinetics in ICR mice indicated that intravenous (i.v.) administration of curcumin/mPEG−PCL−Phe(Boc) micelles could retain curcumin in plasma much better than curcumin/mPEG−PCL micelles. Biodistribution results in Sprague−Dawley rats also showed higher uptake and slower elimination of curcumin into liver, lung, kidney, and brain, and lower uptake into heart and spleen of mPEG−PCL−Phe(Boc) micelles, as compared with mPEG−PCL micelles. Further *in vivo* efficacy evaluation in multidrug-resistant human erythroleukemia K562/ADR xenograft model revealed that i.v. administration of curcumin-loaded mPEG−PCL−Phe(Boc) micelles significantly delayed tumor growth, which was attributed to the improved stability of curcumin in the bloodstream and increased systemic bioavailability. The mPEG−PCL−Phe(Boc) micellar system is promising in overcoming the key challenge of curcumin's to promote its applications in cancer therapy.

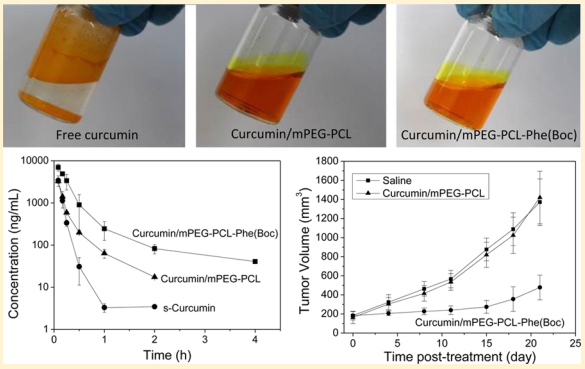

KEYWORDS: *curcumin, polymer micelles, blood-stable, antitumor*

1. INTRODUCTION

As a major cause of mortality worldwide, cancer is a complicated and even unintelligible disease because it develops through multistep carcinogenesis, which involves many cellular physiological systems.[1] Nowadays, despite many advances have been achieved in cancer therapy, chemotherapy is still the most common and widely used procedure in treating human cancers, especially for stage III or stage IV diseases.[2] Frequent limitations encountered by cancer chemotherapy are that the antitumor agents do not distribute specifically or reach adequate concentrations at the tumor site, and/or they have intolerable toxicity.[3,4] Furthermore, tumors are highly aggressive and development of multidrug resistance is also challenging.[5] So developing safe and effective drugs or drug formulations is still at the cutting edge of oncotherapy.

Modern pharmacy and pharmacology have demonstrated that polyphenolic compounds are crucial in preventing diseases and regulating immune system, and many natural products rich of polyphenol have been employed as medicines for these

Special Issue: Polymers in Drug Delivery: Chemistry and Applications

Received: December 28, 2016
Revised: February 14, 2017
Accepted: February 15, 2017
Published: February 15, 2017

DOI: 10.1021/acs.molpharmaceut.6b01171
Mol. Pharmaceutics 2017, 14, 2585−2594

purposes.[6−8] Curcumin, a polyphenolic natural extract of curcuma longa, has many pharmacological effects against oxidant, inflammation, and tumor in various preclinical models.[9−12] Curcumin can down-regulate expression of pro-inflammatory cytokines[13−15] and suppress different cancer types.[16−29] Besides, curcumin also shows great potential in overcoming multidrug resistance[30−32] and a synergistic antitumor effect with other anticancer agents for reducing toxicity and improving efficacy.[33−35] More importantly, curcumin has been confirmed to be well tolerated, bioactive, and innocuous even with a daily intake of 10 g.[36] Nevertheless, clinical applications of curcumin in treating cancers and other diseases are limited because of its water insolubility and rapid degradation at physiological conditions and, consequently, rapid metabolism/excretion and minimal systemic bioavailability.[37] To solve these problems, several approaches have been proposed based on curcumin derivatives, liposomes, nanoparticles, micelles, and prodrugs; however, almost no progress of these formulations in clinical translation has been made until now.[38−44] Among these approaches, self-assembled polymeric micelles have attracted great attention, owing to their readily tailorable chemical structure, high drug loading capacity, and ease for scale-up preparation. With assistance of amphiphilic block copolymers, curcumin can be encapsulated into water-soluble micelles to be completely dispersible in water and intravenously injectable.[45] However, many polymer micelles can be dissociated by the blood components and lose the drug content right after administration.[46−48] In addition, curcumin is quite unstable at psychological conditions. Thus, an efficient curcumin carrier should be able to retain it in blood circulation before it can access the tumor site. For most polymeric micelles, drug encapsulation is mainly based on carrier−drug hydrophobic interaction, which may not provide adequate compatibility for some drug molecules with different hydrophobicity. Therefore, it is critical to choose a suitable hydrophobic block to form the core.[49]

To ensure that the micelle core and the payload therapeutics are more compatible, a simple and effective strategy has been proposed to modify conventional micelle-forming polymers with functional domains that provide additional mechanisms of carrier−drug interactions such as hydrogen bonding, $\pi-\pi$ stacking, and hydrophobic interaction.[50,51] In our previous report, *tert*-butoxycarbonyl (*t*-Boc) containing phenylalanine end-capped mPEG−PLA was found to be quite effective in improving the compatibility between the micelle core and cabazitaxel, resulting in significant improved micelle stability both *in vitro* and *in vivo*.[52] To improve the solubility of curcumin in aqueous solutions and its stability in blood circulation, we have synthesized a block copolymer composed of methoxyl polyethylene glycol (mPEG) and poly(ε-caprolactone) (PCL) end-capped with *N*-(*tert*-butoxycarbonyl)-L-Phenylalanine (Boc−Phe), mPEG−PCL−Phe(Boc), and used it for encapsulation of curcumin. Incorporation of Boc−Phe at the end of the hydrophobic blocks was likely to strengthen carrier−carrier and carrier−drug interaction by intermolecular $\pi-\pi$ stacking of aromatic rings and hydrogen bonding, leading to a more tightly packed core of the micelles. Thus, the micellar nanocarrier can stably retain curcumin in blood circulation and protect it from biotransformation and metabolism to improve its systemic bioavailability.

2. EXPERIMENTAL SECTION

Materials. Curcumin was a gift from Suzhou Nanomedicine Company in Jiangsu with a purity of >99.5%. mPEG with the number-average molecular weight (M_n) of 2000 g/mol, stannous octoate ($Sn(Oct)_2$), ε-caprolactone (CL), dimethyl sulfoxide (DMSO), and 3-(4,5-dimethyl-2-thiazolyl)-2−5-diphenyl tetrazolium bromide (MTT) were products of Sigma-Aldrich (Milwaukee, WI). CL was dried prior to use. Boc−Phe was purchased from GL Biochem in Shanghai, while 4-pyrrolidinopyridine, pivaloyl chloride, and anhydrous dichloromethane (CH_2Cl_2) were from Acros in Beijing. Purchased from Sinopharm Chemical Regent in Shanghai, all other analytical grade chemicals were used as received. Human pancreatic SW1990 cells and multidrug resistant erythroleukemia (K562/ADR) cell line were supplied by the Institute of Biochemistry and Cell Biology, Chinese Academy of Science. Purchased from Vital River Laboratory Animal Technology in Beijing, male ICR mice (6−9 weeks), female BALB/c nude mice (7−9 weeks), and male Sprague−Dawley (SD) rats were used in the animal studies, which were conducted under the protocol approved by the Institutional Animal Care and Use Committee of Soochow University in Suzhou.

Synthesis of mPEG−PCL−Phe(Boc) Diblock Copolymer. As shown in Figure 1, hydroxyl-terminated mPEG−PCL amphiphilic block copolymer was synthesized via ring-opening polymerization of CL in the presence of $Sn(Oct)_2$ as the catalyst and mPEG as the macroinitiator.[53−55] Briefly, mPEG (5 g) was added in a Schlenk bottle and degassed at 130 °C under reduced pressure with magnetic stirring for 3 h. CL (6 g) and $Sn(Oct)_2$ (6 mg) were then added into the bottle, followed by immediate sealing in vacuum and stirring for 24 h at 130 °C. The resulted polymer was dissolved in CH_2Cl_2, concentrated, and then precipitated in cold ether. The resultant precipitate was filtered and dried in vacuum (white powder, yield ~80%), then stored at 4 °C for further use. The terminal hydroxyl group in mPEG−PCL was completely converted into a Boc-protected amino acid without hydrolysis of PCL segments by using a mixed acid anhydride of Boc−Phe with 4-

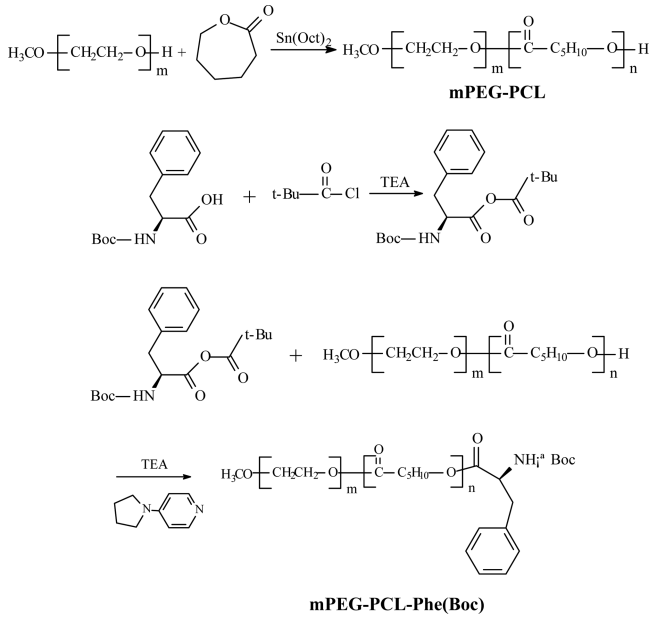

Figure 1. Synthesis of mPEG−PCL−Phe(Boc).

DOI: 10.1021/acs.molpharmaceut.6b01171
Mol. Pharmaceutics 2017, 14, 2585−2594

pyrrolidinopyridine, according to a previous report with modification.[56] Briefly, 6.65 g of Boc−Phe (25 mmol) and 3.5 mL of triethylamine (TEA, 25 mmol) were mixed in a round-bottom flask with 50 mL of dry ethyl acetate. The solution was chilled to −10 °C and added with 3.05 mL of pivaloyl chloride (25 mmol), followed by stirring for 2 h at 0 °C and then for another 1 h at room temperature. After filtration, the solvent was evaporated, and the residue was dried in vacuum. The obtained white solid was redissolved using 25 mL of CH_2Cl_2, and the solution was mixed with mPEG−PCL (20 g), TEA (3.5 mL), and 4-pyrrolidinopyridine (370.5 mg) in 100 mL of chilled CH_2Cl_2. The mixture was stirred for 1 h at 0 °C and then for 6 h at room temperature to complete the reaction. After solvent evaporation, the residue was recrystallized from 100 mL of ethanol three times to afford mPEG−PCL−Phe(Boc) as white powder.

Characterization of the Copolymers. The M_n, weight-average molecular weight M_w, and polydispersity indices (PDI), i.e., M_w/M_n, of the copolymers were determined using gel permeation chromatography (GPC; Waters1515) with tetrahydrofuran (THF) as the eluent. ^{1}H-nuclear magnetic resonance (NMR) spectra were obtained in deuterated chloroform ($CDCl_3$) for confirming the chemical structures and calculating the functionality of terminal hydroxyl groups in mPEG−PCL with Boc−Phe using a Bruker NMR spectrometer (AVANCE III, 500 MHz) at 25 °C. For determining the critical micelle concentration (CMC) of mPEG−PCL−Phe(Boc), the fluorescence spectra of the polymer solutions with pyrene as the probe were recorded using a fluorescence spectrophotometer (RF-5301, Shimadzu) at room temperature. Briefly, 100 μL of pyrene/benzene solution (0.12 mg/mL) was aliquoted into a series of 10 mL volumetric flasks and benzene was evaporated under a blow of N_2. A mPEG−PCL−Phe(Boc) solution in ultrapure water (1 mg/mL) was prepared and diluted in the flasks to a series of concentrations as low as 10 ng/mL.

Preparation and Characterization of Curcumin-Loaded Polymer Micelles. Curcumin-loaded mPEG−PCL−Phe(Boc) micelles were prepared by a convenient method of solid dispersion and thin film hydration.[57] We first dissolved 380 mg of mPEG−PCL−Phe(Boc) and 20 mg of curcumin in 5 mL of absolute ethanol at 50 °C. The solvent was slowly evaporated using a rotary evaporator, and 5 mL of ultrapure water was then added to hydrate the thin film. The formed micelle solution was filtered using a polyvinylidene fluoride (PVDF) filter (0.22 μm, pore size) to remove curcumin that was not encapsulated and then lyophilized. Such a formulation typically contained ∼5% curcumin and ∼95% mPEG−PCL−Phe(Boc). For comparison, we also prepared curcumin/mPEG−PCL and blank mPEG−PCL−Phe(Boc) micelles in the same way. The morphologies of the curcumin-loaded micelles before and after lyophilization were examined using a JEM-2100 transmission electron microscope (TEM; JEOL). The thermal properties of curcumin/mPEG−PCL and curcumin/mPEG−PCL−Phe(Boc) micelles as well as free curcumin were characterized on a differential scanning calorimeter (DSC; DSC-SP, Rheometric Scientific) through a heating cycle from 20 to 200 °C in N_2 at 10 °C/min. The mean diameter of the micelles and their size distribution were determined using dynamic light scattering (DLS; Nicomp 380ZLS, Particle Sizing Systems).

The curcumin concentrations in the micelle solutions were determined at 25 °C using Agilent 1260 high performance liquid chromatography (HPLC). The wavelength (λ) of the detector was 425 nm. The eluent was a mixture of acetonitrile and water (75:25), and the micelle solution was suitably diluted with acetonitrile and filtered using the PVDF filter before it flowed through a SB-C18 chromatographic column at 1 mL/min. Using the formulas given below, we calculated the encapsulation efficiency and loading capacity of the drug. The weight of drug in micelles was derived from the curcumin concentration in the micelle solutions, while the weight of the initial drug included free curcumin that was not encapsulated and later removed before the HPLC determination.

$$\text{encapsulation efficiency}(\%) = \frac{\text{weight of drug in micelles}}{\text{weight of the initial drug}} \times 100$$

$$\text{loading capacity}(\%) = \frac{\text{weight of drug in micelles}}{\text{weight of micelles and drug}} \times 100$$

***In Vitro* Stability of the Reconstituted Polymer Micelles.** We evaluated the *in vitro* stability at 25 °C of curcumin/mPEG−PCL and curcumin/mPEG−PCL−Phe(Boc) micelles in aqueous solutions with the initial curcumin concentration of 4 mg/mL. The mean diameter and polydispersity of the micelles over time were monitored using DLS. The samples (1 mg/mL) in plastic cuvettes were measured in triplicate at λ of 633 nm. The released curcumin crystallized, precipitated, and removed by 10 min centrifugation at 10,000 rpm. Then the curcumin concentrations in the micelle solutions were determined using the HPLC method described in the previous paragraph.

Cytotoxicity Assay. Cytotoxicity of solvent solubilized curcumin in DMSO (s-curcumin), curcumin/mPEG−PCL, and curcumin/mPEG−PCL−Phe(Boc) micelles against human pancreatic SW1990 cell line was analyzed using an MTT assay.[58] Briefly, pancreatic SW1990 cells were cultured in RPMI1640 medium with 15% Fetal Bovine Serum. Then the cells were seeded in 96-well plates (Corning, NY) at 5000 cells/well. After 1 day culture, the cells were exposed to s-curcumin and equivalent amount of curcumin encapsulated in mPEG−PCL and mPEG−PCL−Phe(Boc) micelles reconstituted in saline. The DMSO content in the culture medium was lower than 0.1% to avoid affecting cell proliferation.[59] The vehicle saline was also processed through the MTT assay as the control. After incubation for 1 and 2 days in a Thermo311 incubator, we added 50 μL of MTT solution in PBS into each well and continued the incubation for another 3 h. Then the culture medium was changed using 150 μL of DMSO, followed by thorough agitation for 10 min in a thermo-shaker (MB100−2A, Shanghai) and reading on a SpectraMax 190 microplate reader (Molecular Devices) at λ of 490 nm. The cytotoxicity assay was performed in triplicate and calculated as a percentage of cell apoptosis compared with the control.

Pharmacokinetics and Biodistribution of Curcumin-Loaded Micelles Following Intravenous Administration. We randomly split 63 male ICR mice into three groups (21 for each), receiving s-curcumin (12 mg/mL), curcumin/mPEG−PCL micelles, and curcumin/mPEG−PCL−Phe(Boc) micelles (reconstituted in saline, 12 mg/mL), respectively. Following the intravenous (i.v.) administration of 12 mg/kg of the three curcumin formulations, 0.5 mL of the blood sample was collected from the heart at 5, 10, 15, and 30 min and 1, 2, and 4 h (3 animals for each time point). Then the blood samples were centrifuged for 6 min at 8000 rpm to obtain the plasma

DOI: 10.1021/acs.molpharmaceut.6b01171
Mol. Pharmaceutics 2017, 14, 2585−2594

samples. Then the curcumin concentrations in the plasma samples were analyzed using a liquid chromatograph mass spectrometer (LCMS-2020) equipped with a Shimadzu UV−visible spectrophotometer (Columbia, MD). The detection limitation of the equipment was 1 ng/g. We used the noncompartmental analysis in WinNonlin software V6.2.1 to calculate major pharmacokinetic parameters. The biodistribution study after curcumin i.v. administration was carried out with 18 male SD rats (2 groups, 9 rats for each group). One group received curcumin/mPEG−PCL micelles and the other one received curcumin/mPEG−PCL−Phe(Boc) micelles at a single dosage of 25 mg/kg. After 15 min, 2 h, and 4 h, the animals were sacrificed through cervical dislocation (3 rats at each time point for each group) for collecting tissue samples in heart, liver, spleen, lung, kidney, and brain. These tissue samples were thoroughly washed with ice cold citric acid PBS buffer (pH = 5.7). Then they were blotted dry and weighed before freezing at −80 °C. The curcumin concentrations in the tissue samples were also analyzed using LCMS according to a well-established method.[60] The detection limitation of the equipment was 1 ng/g.

***In Vivo* Antitumor Efficacy.** The therapeutic efficacy of saline and curcumin-loaded mPEG−PCL and mPEG−PCL−Phe(Boc) micelles was examined on nude mice bearing K562/ADR tumor. K562/ADR cells were suspended in RPMI1640 culture medium containing 50% BD Matrigel matrix (No. 356234, BD Biosciences, San Jose). Suspension of 1×10^7 cells in 200 μL medium was injected subcutaneously into animal armpits. Once the mass of the tumor in the xenografts reached 100−200 mm^3, we split the nude mice to three random groups (8 or 10 animals for each) for receiving physiological saline (control), curcumin/mPEG−PCL, and curcumin/mPEG−PCL−Phe(Boc) micelles (i.v., curcumin 40 mg/kg) every day. After the initial treatment, the mice were monitored for 3 weeks in terms of body weight and tumor dimensions (length and width). Tumor volume was calculated using the formula: V = length (cm) × width^2 (cm^2)/2.

Statistical Analysis. The difference between any two treatment groups was determined using the student's t-test or variance analysis (SPSS version 16.0). p values of smaller than 0.05 indicated statistical significance in the differences between two samples.

3. RESULTS AND DISCUSSION

Characteristics of mPEG−PCL−Phe(Boc). mPEG−PCL−Phe(Boc) was prepared and used to encapsulate curcumin for improving its solubility and stability both *in vitro* and *in vivo*. The M_n of mPEG−PCL synthesized in this report was calculated from the ^{1}H NMR spectrum in Figure 2A. The M_n of the PCL block in mPEG−PCL was 1800 g/mol with a PDI of 1.0−1.1. In the second step of end-capping the terminal hydroxyl group with Boc−Phe, the mixed anhydride was found to be a powerful acylating reagent in complete conversion, while it was not detrimental to the polymer backbone, as evidenced in the ^{1}H NMR spectrum (Figure 2B) and GPC analysis (Figure S1). The chemical shift at 3.67 ppm (a) indicated the methene (CH_2) protons in mPEG, while those at 1.40 (b), 1.66 (c), 2.31 (d), and 4.08 (e) ppm belonged to the methene (CH_2) protons in PCL. In comparison with the ^{1}H NMR spectrum of mPEG−PCL, the new chemical shifts at 1.44, 3.10, and 7.15 ppm attributed to the Boc−Phe residue appeared after the coupling reaction, but those for PCL and mPEG still had the same integration ratio, indicating that the

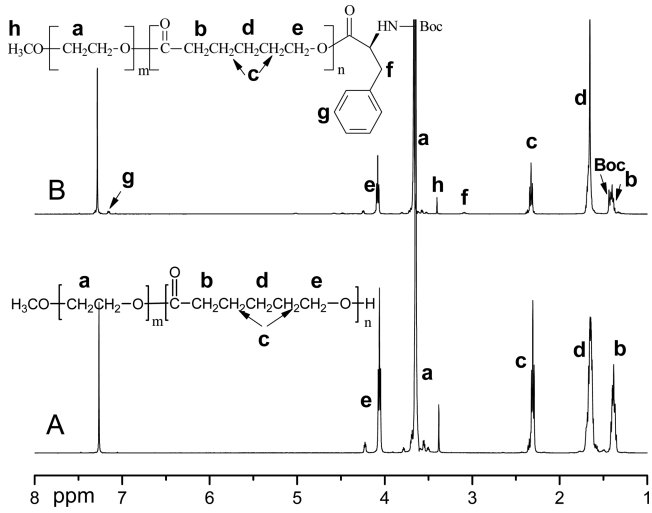

Figure 2. ^{1}H NMR spectra of mPEG−PCL (A) and mPEG−PCL−Phe(Boc) (B).

expected structure formed without other reactions. The ratio of the chemical shift f of the amino acid residue to the chemical shift h of the terminal methyl group in mPEG was used to calculate the average end-capping ratio of mPEG−PCL with Boc−Phe through normalizing the experimental value to the prediction of 2:3 for complete end-capping. The obtained end-capping ratio was always greater than 90%, meaning that almost all the terminal hydroxyl groups were functionalized with Boc−Phe. The GPC traces in Figure S1 also confirmed that by showing a slight increase of 300 g/mol in the polymer molecular weight, while the PDI was almost the same. Based on the intensities of the peaks at λ of 384 and 373 nm in the fluorescence spectra of pyrene in the mPEG−PCL−Phe(Boc) solutions with various polymer concentrations, their ratios (I_{384}/I_{373}) were plotted as a function of polymer concentration on a logarithmic scale, as shown in Figure 3. The I_{384}/I_{373} ratio

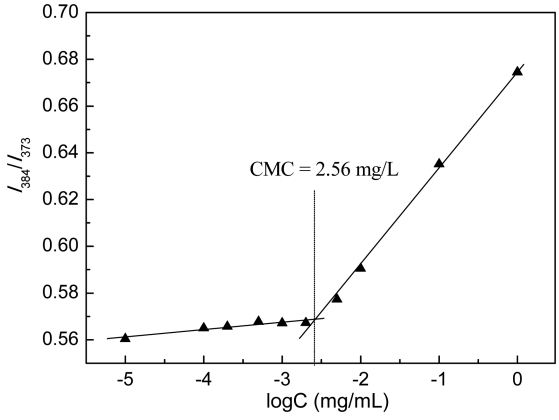

Figure 3. Intensity ratio I_{384}/I_{373} from pyrene excitation spectra as a function of log concentration (mg/mL) of mPEG−PCL−Phe(Boc).

was almost a constant at low concentrations, and then it increased abruptly to indicate that micelles formed. Using the intersection of the tangent to the curve at the inflection with the line through the data at low concentrations, we determined the CMC value to be as low as 2.56 mg/L, suggesting that the copolymer micelles were not sensitive to dilution after administration and had good thermodynamic stability.[61]

DOI: 10.1021/acs.molpharmaceut.6b01171
Mol. Pharmaceutics 2017, 14, 2585−2594

Characteristics of Curcumin-Loaded Polymer Micelles. Curcumin was easily encapsulated in both mPEG−PCL and mPEG−PCL−Phe(Boc) micelles through a facile method that can be easily scaled up.[57] In this process, the amorphous matrix containing curcumin and the polymer self-assembled in water into spherical micelles after the evaporation of the solvent. Hydrophobic curcumin interacted with the hydrophobic micelle core and was trapped there in formation of polymer micelles. The encapsulation efficiency and loading capacity of the prepared curcumin-loaded mPEG−PCL and mPEG−PCL−Phe(Boc) micelles were 98.4 ± 0.42%, 4.76 ± 0.22% and 97.5 ± 0.25%, 4.84 ± 0.13%, respectively. The prepared micelle solution was lyophilized without lyoprotective agents and easy to be reconstituted in aqueous media. As demonstrated in Figure 4, the lyophilized micelles and

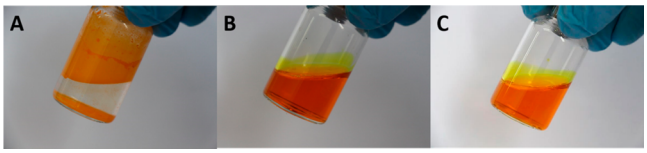

Figure 4. Photos of free curcumin in water (A), curcumin/mPEG−PCL micelles (B), and curcumin/mPEG−PCL−Phe(Boc) micelles (C).

reconstituted micelles were fully dispersed in water to form clear solutions. The micelles in the two curcumin formulations had a regular spherical shape with a narrow distribution, as exemplified using the TEM photographs of curcumin/mPEG−PCL−Phe(Boc) micelles (Figure 5). It can be seen in Figure S2

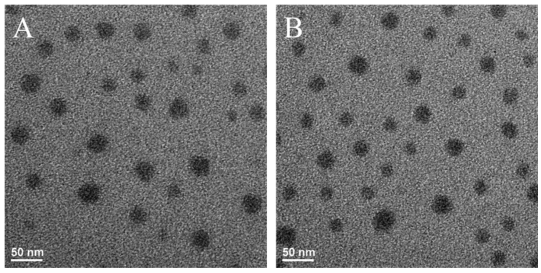

Figure 5. TEM images of curcumin/mPEG−PCL−Phe(Boc) micelles before (A) and after (B) lyophilization.

that the curcumin/mPEG−PCL−Phe(Boc) micelle size was ∼23 nm with a DLS polydispersity less than 0.1, slightly smaller than curcumin/mPEG−PCL micelles (∼25 nm with a polydispersity less than 0.1), indicating a more tightly packed core of curcumin-encapsulated mPEG−PCL−Phe(Boc) micelles. No significant difference was observed for the micelle diameter before and after lyophilization, meaning that the two curcumin formulations were both stable in the process.

The thermal properties of free curcumin, curcumin/mPEG−PCL, and curcumin/mPEG−PCL−Phe(Boc) micelles are shown in the DSC curves (Figure S3). The melting point of curcumin was measured to be ∼182 °C. While in the DSC curve of curcumin/mPEG−PCL and curcumin/mPEG−PCL−Phe(Boc) micelles, the intrinsic melting peak of curcumin vanished, indicating that all curcumin has been molecularly incorporated into the core of the micelles. This result also explained well that micelle encapsulation could greatly enhance the solubility of curcumin.

***In Vitro* Stability of the Reconstituted Polymer Micelles.** The *in vivo* performance of the drug-loaded micelles including biodistribution and tumor targeting is closely related to their stability, which is in turn determined majorly by the interaction between the drug and its hydrophobic environment, i.e., the micelle core. In contrast, for polymer micelles without encapsulated drug, the stability mainly depends on the CMC value. To compare the *in vitro* stability between curcumin/mPEG−PCL micelles and curcumin/mPEG−PCL−Phe(Boc) micelles, we incubated these two kinds of micellar curcumin in aqueous solutions at 25 °C and analyzed their size, polydispersity, and curcumin concentration changes over time using both DLS and HPLC. The hydrophobic core of mPEG−PCL micelles seemed not to have sufficiently strong interaction with curcumin to hold it. As demonstrated in Figure 6, the curcumin/mPEG−PCL micelle diameter and its polydispersity both increased significantly on the first day of incubation at 25 °C, and curcumin precipitated in the solution could be observed. At day 3, the mean diameter and polydispersity increased to ∼35 nm and 0.33, respectively. Correspondingly, curcumin remained solubilized in the solution was determined to be less than 70% of the initial concentration. In contrast, the mean diameter and polydispersity of curcumin/mPEG−PCL−Phe(Boc) micelles and the curcumin concentration in the solution did not change significantly in the first 2 weeks. Even at week 4, the curcumin concentration in the solution was still ∼90% of the initial value though the curcumin precipitate was evident. In addition, curcumin/mPEG−PCL−Phe(Boc) micelle solution was found to be quite stable at 4 °C as the micelles and curcumin concentration remained intact even after several months. The above results indicated that besides hydrophobic interaction, $\pi-\pi$ stacking, and hydrogen bonding obviously impacted the overall carrier−drug interaction. The Boc−Phe residue in mPEG−PCL−Phe(Boc) contained one $\pi-\pi$ stacking aromatic ring and one hydrogen bonding donor/acceptor, leading to a much stronger carrier−drug interaction than the terminal hydroxyl group in mPEG−PCL.

***In Vitro* Cytotoxicity.** To investigate the difference between the two nanocarrier formulations in delivering hydrophobic curcumin to cancer cells, we performed a comparative cytotoxicity study using human pancreatic SW1990 cell line and a control group of s-curcumin. As shown in Figure 7, curcumin-loaded micelles showed equal cytotoxicity compared with s-curcumin at low concentrations, in agreement with the cell images (data not shown). The half maximal inhibitory concentrations (IC_{50}) for s-curcumin and micellar curcumin were found to be 22−25 μg/mL. While at high concentrations of 80 and 100 μg/mL, free curcumin dissolved in DMSO easily precipitated in the culture media, obviously affecting the drug uptake by cancer cells. s-Curcumin showed lower cytoxicity as compared with curcumin-loaded micelles at high concentrations. No significant difference in cytotoxicity was seen in the curcumin nanocarrier formulations against SW1990 cell line. In other words, mPEG−PCL−Phe(Boc) micelles enhanced the solubility of curcumin effectively and provided a convenient method for cellular uptake. In clear contrast, mPEG−PCL−Phe(Boc) micelles containing no curcumin showed little cytotoxicity even at a polymer concentration of 1900 μg/mL.

Pharmacokinetics and Biodistribution. Polymeric micelles are advantageous carriers for delivering hydrophobic drugs through parenteral administration because they are less toxic while better drug solubility and tissue penetration. Many polymeric micelles, however, were found to immediately lose

DOI: 10.1021/acs.molpharmaceut.6b01171
Mol. Pharmaceutics 2017, 14, 2585−2594

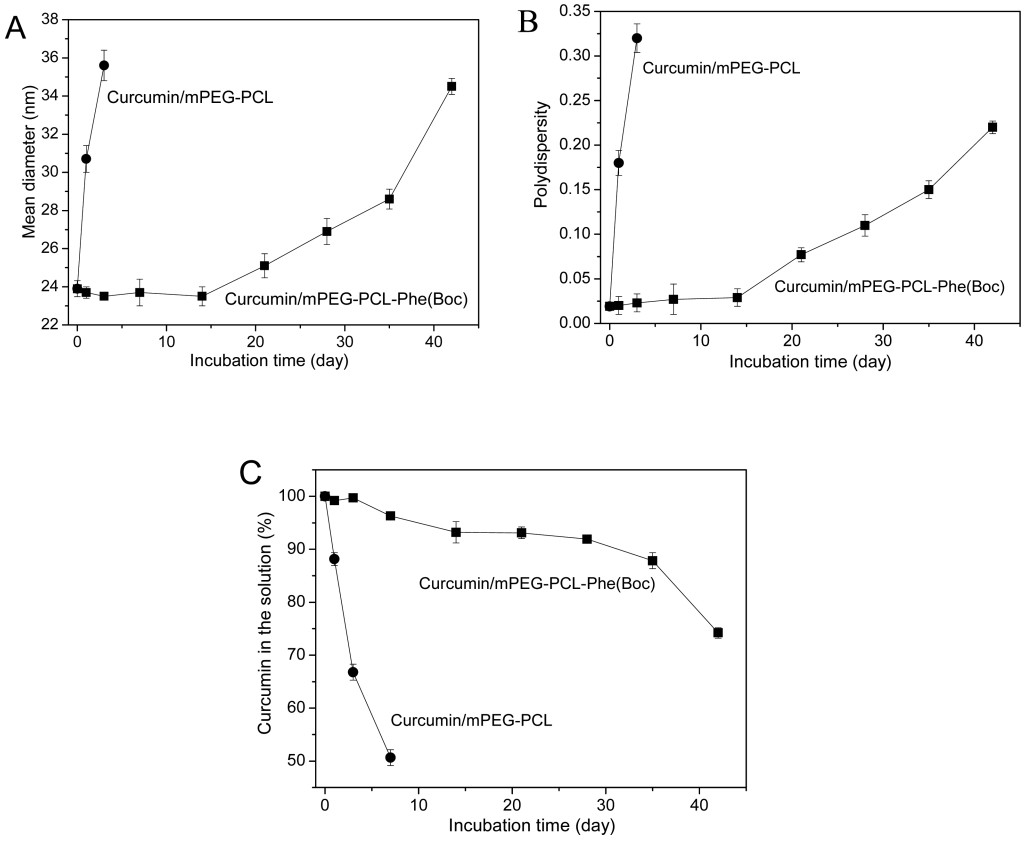

Figure 6. Mean diameter (A) and polydispersity (B) of curcumin/mPEG−PCL and curcumin/mPEG−PCL−Phe(Boc) micelles and the fraction of curcumin remained in the micellar solution (C) as a function of incubation time in aqueous solution at 25 °C. Initial curcumin concentration: 4 mg/mL.

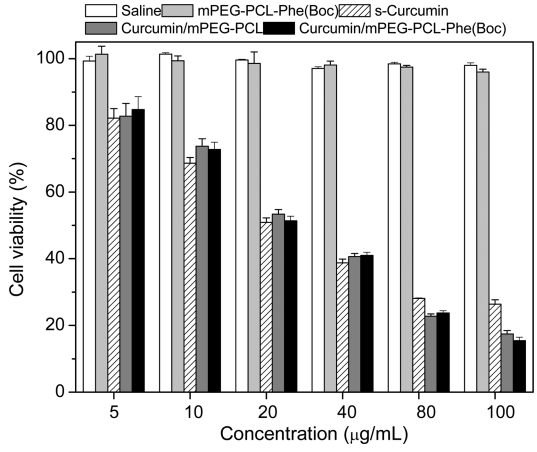

Figure 7. SW1990 cell viability after incubation with free curcumin, curcumin/mPEG−PCL, and curcumin/mPEG−PCL−Phe(Boc) micelles at various concentrations for 2 days.

the drug content upon systemic administration as they were not sufficiently stable at psychological conditions.[46,62,63] Since free curcumin in the blood circulation was subjected to rapid metabolism and elimination by the liver,[64] one of the most important "pre-requisites" in the design of an efficient curcumin carrier is to stably retain it in the blood circulation for a prolonged duration before accessing normal tissues and the tumor site.

The curcumin/mPEG−PCL−Phe(Boc) micellar formulation was superior in its excellent stability that can protect the curcumin payload in the micelle core from metabolism and elimination and therefore prolong the circulation time after systemic administration. But note that *in vitro* result on a drug delivery system cannot represent its *in vivo* performance. Oftentimes, it is difficult to have long drug circulation as the result of rapid partitioning between the drug and the carrier after administration.[65] Curcumin/mPEG−PCL−Phe(Boc) micelles were designed to protect curcumin from fast metabolism and elimination and thus to improve the systemic bioavailability.[37] In the present report, a comparative study of pharmacokinetics and tissue distribution among free s-curcumin, curcumin-loaded mPEG−PCL, and mPEG−PCL−Phe(Boc) micelles after i.v. administration in ICR mice and SD rats were performed. The main pharmacokinetic parameters of these three formulations in Table 1 were calculated using noncompartmental analysis.

Figure 8 shows that the curcumin levels in plasma of ICR mice from s-curcumin and curcumin/mPEG−PCL micelles declined rapidly and became lower than the detection limitation of 1 ng/mL after 4 h. Moreover, for these two curcumin formulations and the single dosage of 12 mg/kg, the curcumin concentration in plasma was for no more than 1 h at the level over 100 ng/mL. The curcumin levels in plasma were sustained not sufficiently long for being effective against cancers. A distinct result was found in the group treated with curcumin/mPEG−PCL−Phe(Boc) micelles. The curcumin levels in plasma declined rapidly (but not as rapid as the other two formulations) in the first hour, followed by a slow decrease. In addition, the concentrations of curcumin in plasma were much higher than those of the groups treated with s-curcumin and

DOI: 10.1021/acs.molpharmaceut.6b01171
Mol. Pharmaceutics 2017, 14, 2585−2594

Table 1. Pharmacokinetic Parameters after i.v. Administration of s-Curcumin, Curcumin/mPEG−PCL, and Curcumin/mPEG−PCL−Phe(Boc) Micelles in ICR Mice at a Single Dosage of 12 mg/kg

parameters	s-curcumin	curcumin/mPEG−PCL	curcumin/mPEG−PCL−Phe(Boc)
$AUC_{(0\text{-}t)}$ (μg/L·h)	877.00	931.34	2657.11
$AUC_{(0\text{-}\infty)}$ (μg/L·h)	877.67	942.49	2730.02
$t_{1/2}$ (h)	0.19	0.44	1.24
C_{max} (ng/L)	3431.56	3272.41	7006.61
V_z (L/kg)	3.79	8.1	7.83
CL_z (L/h/kg)	13.67	12.73	4.40
$MRT_{(0\text{-}\infty)}$ (h)	0.08	0.21	0.53

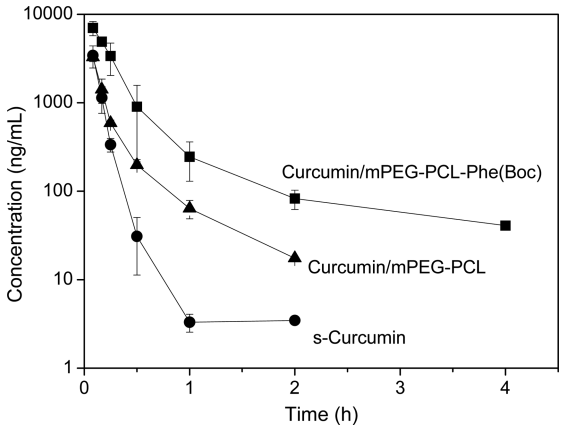

Figure 8. Plasma concentration−time curves after i.v. administration of s-curcumin (dissolved in DMSO), curcumin/mPEG−PCL, and curcumin/mPEG−PCL−Phe(Boc) micelles in ICR mice at a single dosage of 12 mg/kg.

curcumin/mPEG−PCL micelles at all the time points. Even after 4 h, the curcumin concentration in plasma from the group treated with curcumin/mPEG−PCL−Phe(Boc) micelles was still ~40 ng/mL, which was equal to that value upon receiving a daily oral intake of 10 g.[36] It is possible that the mPEG−PCL−Phe(Boc) micellar formulation of curcumin was resistant to liver metabolism so that the curcumin concentration in plasma declined more gradually than the other two: s-curcumin and curcumin/mPEG−PCL micelles. The area under the time−concentration curve (AUC) was 2.90-fold larger, the half-life of elimination ($t_{1/2}$) was 2.82-fold longer, the mean residence time (MRT) was 2.52-fold longer, the maximum concentration in plasma was 2.14-fold higher in the curcumin/mPEG−PCL−Phe(Boc) micellar formulation, relative to curcumin/mPEG−PCL micelles. Meanwhile, the total body clearance (CL_z) were significantly lower, indicating that encapsulating curcumin in mPEG−PCL−Phe(Boc) micelles was efficient to reduce its elimination from the body. Taken together, we can conclude that the curcumin/mPEG−PCL−Phe(Boc) micellar formulation promoted its stability in blood circulation and consequently its bioavailability *in vivo*, as the encapsulated curcumin was protected from metabolism.

How curcumin distributes in body tissues after i.v. administration is crucial for its biological activity; however, this issue has not been well understood.[66] Toward evaluating the tissue distribution profiles of the present micellar systems, curcumin-loaded mPEG−PCL and mPEG−PCL−Phe(Boc) micelles were i.v. administered in SD rats at 25 mg/kg. As shown in Figure 9, both nanocarrier formulations demonstrated

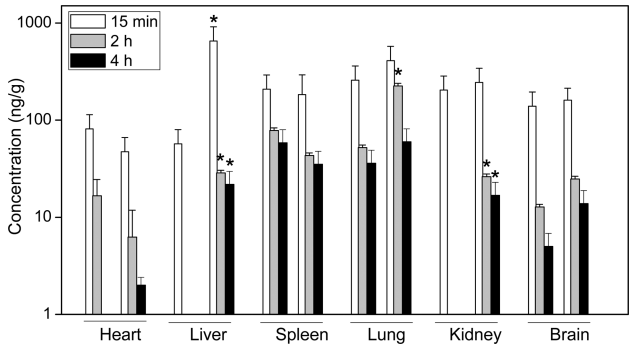

Figure 9. Curcumin distribution in tissues after i.v. administration of curcumin/mPEG−PCL (left) and curcumin/mPEG−PCL−Phe(Boc) (right) micelles in SD rats at a single dosage of 25 mg/kg. $p < 0.05$ relative to the curcumin/mPEG−PCL group at the same time point.

rapid curcumin distribution into most tissues within 15 min. However, the drug in the residual blood affected the quantification of drugs in organs. Generally, curcumin/mPEG−PCL−Phe(Boc) micelles significantly improved the curcumin accumulation in liver, lung, and kidney, and reduced curcumin distribution in heart, spleen, and brain, compared with curcumin/mPEG−PCL micelles. The preferred accumulation of drug in liver, kidney, and lung might be partly due to the longer blood circulation of the drug formulation. Our results also clearly demonstrated that the major difference in tissue distribution in SD rats between these two micellar formulations was in liver and kidney, where curcumin was metabolized and eliminated.[64] The curcumin level in liver from curcumin/mPEG−PCL−Phe(Boc) micelle group was 651.67 ng/g at 15 min and then decreased rapidly to 28.58 ng/g at 2 h, followed by a slow and steady decrease reaching 21.8 ng/g after 4 h. In contrast, curcumin/mPEG−PCL micelles showed much lower and shorter distribution in that curcumin was detected only at 15 min at a level of 57.1 ng/g and became lower than the detection limitation of 1 ng/g at 2 h. Curcumin distribution in kidney from these two formulations showed a quite similar trend as in liver although the curcumin levels were almost the same at 15 min after administration. The metabolites of curcumin in rodents and humans are known to subject to conjugations like sulfation and glucuronidation, and liver is the main organ responsible for curcumin metabolism.[64,67] Results from this study provided solid evidence that the blood-stable micelles effectively protected the encapsulated curcumin from metabolism and elimination by liver and kidney.

Figure 9 shows that the curcumin accumulation in lung was also significantly higher upon receiving curcumin/mPEG−PCL−Phe(Boc) micelles, compared with the group treated with curcumin/mPEG−PCL micelles. The accumulation in lung occurred when pulmonary capillary beds filtered after i.v. administration of blood-stable curcumin-loaded micelles. For nanocarrier drug delivery system, long circulation of the drug is usually achieved by reducing phagocytic cell uptake, which most probably happens in spleen. To support this observation, we further analyzed the curcumin concentrations in spleen (Figure 9). No significant difference was seen in the curcumin concentration in spleen between these two formulations, although the values were slightly lower in the curcumin/mPEG−PCL−Phe(Boc) micelle group. The relative lower levels amassed in spleen might result from the decreased phagocytic cell uptake in the reticuloendothelial system. Despite the relatively prolonged retention time, the curcumin

DOI: 10.1021/acs.molpharmaceut.6b01171
Mol. Pharmaceutics 2017, 14, 2585−2594

accumulation in heart was also lower in the group receiving curcumin/mPEG−PCL−Phe(Boc) micelles than the curcumin/mPEG−PCL group, indicating that curcumin-loaded micelles were less effective on heart than on other tissues.

In recent years, curcumin has demonstrated the feasibility of impeding the progress of Alzheimer's disease.[68] However, there lacks therapeutic effect from conventional curcumin in treating patients with Alzheimer's disease and the short systemic retention of curcumin in brain might be the reason. Unfortunately, in the present study, blood stable curcumin/mPEG−PCL−Phe(Boc) micelles seemed to be ineffective in improving the curcumin level in brain as compared with blood unstable curcumin/mPEG−PCL micelles. There was a trend that mPEG−PCL−Phe(Boc) micelles slightly decreased the curcumin level in brain than mPEG−PCL micelles, although this was not significant. For this reason, the blood-stable micellar curcumin was thought to be not advantageous to other conventional curcumin formulations in treating brain diseases.

Antitumor Efficacy. We studied the *in vivo* antitumor efficacy of curcumin/mPEG−PCL and curcumin/mPEG−PCL−Phe(Boc) micelles using K562/ADR human erythroleukemia xenograft tumor model in nude mice, with the aim for evaluating whether blood-stable curcumin formulation generated superior antitumor efficacy compared with a less stable curcumin formulation. The mice were treated with these two micellar curcumin formulations (40 mg/kg, dosage) and administered every day for three consecutive weeks. As shown in Figure 10A,B, saline and less-stable curcumin/mPEG−PCL micelles were ineffective in inhibiting the tumor growth. In clear contrast, blood-stable curcumin/mPEG−PCL−Phe(Boc) micelles significantly delayed the tumor growth. The corresponding tumor growth inhibition (TGI) and tumor weight for the mice receiving the treatment of curcumin/mPEG−PCL and curcumin/mPEG−PCL−Phe(Boc) micelles at day 21 were −9.5%, 0.79 ± 0.28 g and 65.1%, 0.39 ± 0.26 g, respectively. Inhibition of the tumor growth by blood-stable curcumin/mPEG−PCL−Phe(Boc) micelles was much more efficient than by curcumin/mPEG−PCL micelles. Figure 10C showed the changes in the body weights of the mice treated with different curcumin formulations. Body weight variation during the treatment normally can be considered as an indicator of the adverse effects and toxicity of the formulations. In the present study, the body weight loss was no more than 10% for these two micellar curcumin formulations relative to the control group treated with saline, suggesting no severe systemic toxicity of curcumin.

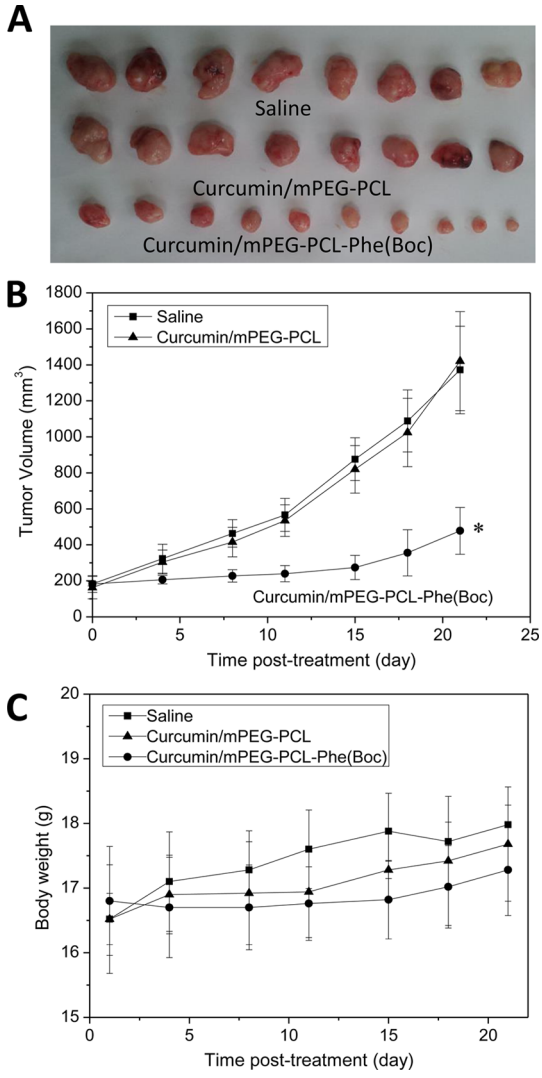

Figure 10. *In vivo* antitumor efficacy. (A) Photos of K562/ADR tumors after 21 days and (B) tumor growth curves in different groups after treatments. Each point represents the mean of tumor volume ± standard error of the mean (SEM). (B) Body weights of mice after various treatments. Values are means ± SEM; $p < 0.05$ relative to the groups treated with saline and curcumin/mPEG−PCL micelles.

4. CONCLUSIONS

We have developed a blood-stable mPEG−PCL−Phe(Boc) polymeric micellar formulation for curcumin delivery and its pharmacokinetics, biodistribution, and antitumor efficacy have been evaluated. This micellar formulation stably retained curcumin in blood circulation against metabolism and elimination, and improved curcumin accumulation into liver, lung, kidney, and brain, while decreasing curcumin distribution into heart and spleen compared with less stable mPEG−PCL micellar system. Findings in the tumor growth inhibition study further confirmed the potential role of curcumin in treating multidrug resistant erythroleukemia. Therefore, the micellar system developed here is expected to find future uses for delivering curcumin for improving the antitumor efficacy and preventing toxicity in traditional chemotherapy as well as overcome multidrug resistance. The present study also highlighted the importance of stability of the drug carrier when they were used for *in vivo* delivery of curcumin.

■ ASSOCIATED CONTENT

Supporting Information

The Supporting Information is available free of charge on the ACS Publications website at DOI: 10.1021/acs.molpharmaceut.6b01171.

GPC curves of mPEG−PCL and mPEG−PCL−Phe(Boc); particle size distribution of curcumin/mPEG−PCL and curcumin/mPEG−PCL−Phe(Boc) micelles before and after lyophilization; DSC curves of free curcumin, curcumin/mPEG−PCL, and curcumin/mPEG−PCL−Phe(Boc) micelles (PDF)

■ AUTHOR INFORMATION

Corresponding Authors

*(J.L.) Tel: +86 0532 82913125. Fax: +86 0532 82913126.

DOI: 10.1021/acs.molpharmaceut.6b01171
Mol. Pharmaceutics 2017, 14, 2585−2594

*(S.W.) Tel: +1 865 974 7809. Fax: +1 865 974 4115.

ORCID

Shanfeng Wang: 0000-0001-9790-5970

Author Contributions

⊥These authors contributed equally to this study.

Notes

The authors declare no competing financial interest.

■ ACKNOWLEDGMENTS

The authors thank the financial support from the National Science & Technology Major Projects (China) for Major New Drugs Innovation & Development (No. 2014-ZX09301306-006).

■ REFERENCES

(1) Reichert, J. M.; Wenger, J. B. Development trends for new cancer therapeutics and vaccines. *Drug Discovery Today* **2008**, *13*, 30−37.

(2) Singhal, S.; Nie, S. M.; Wang, M. D. Nanotechnology applications in surgical oncology. *Annu. Rev. Med.* **2010**, *61*, 359−373.

(3) Misra, R.; Acharya, S.; Sahoo, S. K. Cancer nanotechnology: application of nanotechnology in cancer therapy. *Drug Discovery Today* **2010**, *15*, 842−850.

(4) Das, M.; Mohanty, C.; Sahoo, S. K. Ligand-based targeted therapy for cancer tissue. *Expert Opin. Drug Delivery* **2009**, *6*, 285−304.

(5) Parveen, S.; Sahoo, S. K. Polymeric nanoparticles for cancer therapy. *J. Drug Target* **2008**, *16*, 108−123.

(6) Conney, A. H. Enzyme induction and dietary chemicals as approaches to cancer chemoprevention: the Seventh DeWitt S. Goodman Lecture. *Cancer Res.* **2003**, *63*, 7005−7031.

(7) Yang, F. S.; Lim, G. P.; Begum, A. N.; Ubeda, O. J.; Simmons, M. R.; Ambegaokar, S. S.; Chen, P. P.; Kayed, R.; Glabe, C. G.; Frautschy, S. A.; Cole, G. M. Curcumin inhibits formation of amyloid β oligomers and fibrils, binds plaques, and reduces amyloid *in vivo*. *J. Biol. Chem.* **2005**, *7*, 5892−5901.

(8) Ono, K.; Hasegawa, K.; Naiki, H.; Yamada, M. Curcumin has potent anti-amyloidogenic effects for Alzheimer's β-amyloid fibrils *in vitro*. *J. Neurosci. Res.* **2004**, *75*, 742−750.

(9) Basnet, P.; Skalko-Basnet, N. Curcumin: an anti-inflammatory molecule from a curry spice on the path to cancer treatment. *Molecules* **2011**, *16*, 4567−4598.

(10) Kanai, M.; Yoshimura, K.; Asada, M.; Imaizumi, A.; Suzuki, C.; Matsumoto, S.; Nishimura, T.; Mori, Y.; Masui, T.; Kawaguchi, Y.; Yanagihara, K.; Yazumi, S.; Chiba, T.; Guha, S.; Aggarwal, B. B. A phase I/II study of gemcitabine-based chemotherapy plus curcumin for patients with gemcitabine-resistant pancreatic cancer. *Cancer Chemother. Pharmacol.* **2011**, *68*, 157−164.

(11) Dhillon, N.; Aggarwal, B. B.; Newman, R. A.; Wolff, R. A.; Kunnumakkara, A. B.; Abbruzzese, J. L. Phase II trial of curcumin in patients with advanced pancreatic cancer. *Clin. Cancer Res.* **2008**, *14*, 4491−4499.

(12) Aggarwal, B. B.; Harikumar, K. B. Potential therapeutic effects of curcumin, the anti-inflammatory agent, against neurodegenerative, cardiovascular, pulmonary, metabolic, autoimmune and neoplastic. Int. *Int. J. Biochem. Cell Biol.* **2009**, *41*, 40−59.

(13) Goel, A.; Kunnumakkara, A. B.; Aggarwal, B. B. Curcumin as "Curecumin": from kitchen to clinic. *Biochem. Pharmacol.* **2008**, *75*, 787−809.

(14) Egan, M. E.; Pearson, M.; Weiner, S. A.; Rajendran, V.; Rubin, D.; Glöckner-Pagel, J.; Canny, S.; Du, K.; Lukacs, G. L.; Caplan, M. J. Curcumin, a major constituent of turmeric, corrects cystic fibrosis defects. *Science* **2004**, *304*, 600−602.

(15) Maheshwari, R. K.; Singh, A. K.; Gaddipati, J.; Srimal, R. C. Multiple biological activities of curcumin: a short review. *Life Sci.* **2006**, *78*, 2081−2087.

(16) Dorai, T.; Cao, Y. C.; Dorai, B.; Buttyan, R.; Katz, A. E. Therapeutic potential of curcumin in human prostate cancer. III. Curcumin inhibits proliferation, induces apoptosis, and inhibits angiogenesis of LNCaP prostate cancer cells *in vivo*. *Prostate* **2001**, *47*, 293−303.

(17) Pan, M. H.; Chang, W. L.; Lin-Shiau, S. Y.; Ho, C. T.; Lin, J. K. Induction of apoptosis by garcinol and curcumin through cytochrome c release and activation of caspases in human leukemia HL-60 cells. *J. Agric. Food Chem.* **2001**, *49*, 1464−1474.

(18) Tian, B. Q.; Wang, Z. P.; Zhao, Y. M.; Wang, D. G.; Li, Y. G.; Ma, L.; Li, X. M.; Li, J.; Xiao, N.; Tian, J. Q.; Rodriguez, R. Effects of curcumin on bladder cancer cells and development of urothelial tumors in a rat bladder carcinogenesis model. *Cancer Lett.* **2008**, *264*, 299−308.

(19) Kuo, M. L.; Huang, T. S.; Lin, J. K. Curcumin, an antioxidant and anti-tumor promoter, induces apoptosis in human leukemia cells. *Biochim. Biophys. Acta, Mol. Basis Dis.* **1996**, *1317*, 95−100.

(20) Kunnumakkara, A. B.; Guha, S.; Krishnan, S.; Diagaradjane, P.; Gelovani, J.; Aggarwal, B. B. Curcumin potentiates antitumor activity of gemcitabine in an orthotopic model of pancreatic cancer through suppression of proliferation, angiogenesis, and inhibition of nuclear factor-κB−regulated gene products. *Cancer Res.* **2007**, *67*, 3853−3861.

(21) Dandekar, P.; Jain, R.; Kumar, C.; Subramanian, S.; Samuel, G.; Venkatesh, M.; Patravale, V. Curcumin loaded pH-sensitive nanoparticles for the treatment of colon cancer. *J. Biomed. Nanotechnol.* **2009**, *5*, 445−455.

(22) Zhang, F.; Altorki, N. K.; Mestre, J. R.; Subbaramaiah, K.; Dannenberg, A. J. Curcumin inhibits cyclooxygenase-2 transcription in bile acid- and phorbol ester-treated human gastrointestinal epithelial cells. *Carcinogenesis* **1999**, *20*, 445−451.

(23) Bush, J. A.; Cheung, K. J., Jr; Li, G. Curcumin induces apoptosis in human melanoma cells through a Fas receptor/caspase-8 pathway independent of p53. *Exp. Cell Res.* **2001**, *271*, 305−314.

(24) Choudhuri, T.; Pal, S.; Agwarwal, M. L.; Das, T.; Sa, G. Curcumin induces apoptosis in human breast cancer cells through p53-dependent Bax induction. *FEBS Lett.* **2002**, *512*, 334−340.

(25) Bondi, M. L.; Craparo, E. F.; Picone, P.; Di, C. M.; Di, G. R.; Capuano, G.; Giammona, G. Curcumin entrapped into lipid nanosystems inhibits neuroblastoma cancer cell growth and activates Hsp70 protein. *Curr. Nanosci.* **2010**, *6*, 439−445.

(26) Mukhopadhyay, A.; Bueso-Ramos, C.; Chatterjee, D.; Pantazis, P.; Aggarwal, B. B. Curcumin downregulates cell survival mechanisms in human prostate cancer cell lines. *Oncogene* **2001**, *20*, 7597−7609.

(27) Han, S.; Chung, S.; Robertson, D. A.; Ranjan, D.; Bondada, S. Curcumin causes the growth arrest and apoptosis of B cell lymphoma by downregulation of egr-1, c-myc, bcl-X L, NF-κB, and p53. *Clin. Immunol.* **1999**, *93*, 152−161.

(28) Lev-Ari, S.; Vexler, A.; Starr, A.; Ashkenazy-Voghera, M.; Greif, J.; Aderka, D.; Ben-Yosef, R. Curcumin augments gemcitabine cytotoxic effect on pancreatic adenocarcinoma cell lines. *Cancer Invest.* **2007**, *25*, 411−418.

(29) Darvesh, A. S.; Aggarwal, B. B.; Bishayee, A. Curcumin and liver cancer: a review. *Curr. Pharm. Biotechnol.* **2012**, *13*, 218−228.

(30) Tang, X. Q.; Bi, H.; Feng, J. Q.; Cao, J. G. Effect of curcumin on multidrug resistance in resistant human gastric carcinoma cell line SGC7901/VCR. *Acta Pharmacol. Sin.* **2005**, *26*, 1009−1016.

(31) Weir, N. M.; Selvendiran, K.; Kutala, V. K.; Tong, L.; Vishwanath, S.; Rajaram, M.; Tridandapani, S.; Anant, S.; Kuppusamy, P. Curcumin induces G2/M arrest and apoptosis in cisplatin-resistant human ovarian cancer cells by modulating Akt and p38 MAPK. *Cancer Biol. Ther.* **2007**, *6*, 178−184.

(32) Hu, C. J.; Zhang, L. Nanoparticle-based combination therapy toward overcoming drug resistance in cancer. *Biochem. Pharmacol.* **2012**, *83*, 1104−1111.

(33) Verma, S. P.; Salamone, E.; Goldin, B. Curcumin and genistein, plant natural products, show synergistic inhibitory effects on the growth of human breast cancer MCF-7 cells induced by estrogenic pesticides. *Biochem. Biophys. Res. Commun.* **1997**, *233*, 692−696.

(34) Khafif, A.; Schantz, S. P.; Chou, T. C.; Edelstein, D.; Sacks, P. G. Quantitation of chemopreventive synergism between (−)-epigallocatechin-3-gallate and curcumin in normal, premalignant and malignant human oral epithelial cells. *Carcinogenesis* **1998**, *19*, 419−424.

DOI: 10.1021/acs.molpharmaceut.6b01171
Mol. Pharmaceutics 2017, 14, 2585−2594

(35) Ganta, S.; Amiji, M. Coadministration of paclitaxel and curcumin in nanoemulsion formulations to overcome multidrug resistance in tumor cells. *Mol. Pharmaceutics* **2009**, *6*, 928−939.
(36) Cheng, A. L.; Hsu, C. H.; Lin, J. K.; Hsu, M. M.; Ho, Y. F.; Shen, T. S.; Ko, J. Y.; Lin, J. T.; Lin, B. R.; Ming-Shiang, W.; Yu, H. S.; Jee, S. H.; Chen, G. S.; Chen, T. M.; Chen, C. A.; Lai, M. K.; Pu, Y. S.; Pan, M. H.; Wang, Y. J.; Tsai, C. C.; Hsieh, C. Y. Phase I clinical trial of curcumin, a chemopreventive agent, in patients with high-risk or pre-malignant lesions. *Anticancer Res.* **2001**, *21*, 2895−2900.
(37) Anand, P.; Kunnumakkara, A. B.; Newman, R. A.; Aggarwal, B. B. Bioavailability of curcumin: problems and promises. *Mol. Pharmaceutics* **2007**, *4*, 807−818.
(38) Basile, V.; Ferrari, E.; Lazzari, S.; Belluti, S.; Pignedoli, F.; Imbriano, C. Curcumin derivatives: molecular basis of their anti-cancer activity. *Biochem. Pharmacol.* **2009**, *78*, 1305−1315.
(39) Nurfina, A. N.; Reksohadiprodjo, M. S.; Timmerman, H.; Jenie, U. A.; Sugiyanto, D.; van der Goot, H. Synthesis of some symmetrical curcumin derivatives and their antiinflammatory activity. *Eur. J. Med. Chem.* **1997**, *32*, 321−328.
(40) Safavy, A.; Raisch, K. P.; Mantena, S.; Sanford, L. L.; Sham, S. W.; Krishna, N. R.; Bonner, J. A. Design and development of water-soluble curcumin conjugates as potential anticancer agents. *J. Med. Chem.* **2007**, *50*, 6284−6288.
(41) Nicolas, J.; Mura, S.; Brambilla, D.; Mackiewicz, N.; Couvreur, P. Design, functionalization strategies and biomedical applications of targeted biodegradable/biocompatible polymer-based nanocarriers for drug delivery. *Chem. Soc. Rev.* **2013**, *42*, 1147−1235.
(42) Bansal, S. S.; Goel, M.; Aqil, F.; Vadhanam, M. V.; Gupta, R. C. Advanced drug delivery systems of curcumin for cancer chemoprevention. *Cancer Prev. Res.* **2011**, *4*, 1158−1171.
(43) Kaditi, E.; Mountrichas, G.; Pispas, S. Amphiphilic block copolymers by a combination of anionic polymerization and selective post-polymerization functionalization. *Eur. Polym. J.* **2011**, *47*, 415−434.
(44) Sun, Q.; Radosz, M.; Shen, Y. Challenges in design of translational nanocarriers. *J. Controlled Release* **2012**, *164*, 156−169.
(45) Shahani, K.; Swaminathan, S. K.; Freeman, D.; Blum, A.; Ma, L.; Panyam, J. Injectable sustained release microparticles of curcumin: a new concept for cancer chemoprevention. *Cancer Res.* **2010**, *70*, 4443−4452.
(46) Savic, R.; Azzam, T.; Eisenberg, A.; Maysinger, D. Assessment of the integrity of poly (caprolactone)-*b*-poly(ethylene oxide) micelles under biological conditions: a fluorogenic-based approach. *Langmuir* **2006**, *22*, 3570−3578.
(47) Chen, H.; Kim, S.; He, W.; Wang, H.; Low, P. S.; Park, K.; Chen, J. X. Fast release of lipophilic agents from circulating PEG-PDLLA micelles revealed by *in vivo* forster resonance energy transfer imaging. *Langmuir* **2008**, *24*, 5213−5217.
(48) Letchford, K.; Burt, H. M. Copolymer micelles and nanospheres with different *in vitro* stability demonstrate similar paclitaxel pharmacokinetics. *Mol. Pharmaceutics* **2012**, *9*, 248−260.
(49) Carstensa, M. G.; de Jong, P. H. J. L. F.; van Nostrum, C. F.; Kemmink, J.; Verrijk, R.; de Leede, L. G. J.; Crommeli, D.; Hennink, W. E. The effect of core composition in biodegradable oligomeric micelles as taxane formulations. *Eur. J. Pharm. Biopharm.* **2008**, *68*, 596−606.
(50) Gao, X.; Huang, Y. X.; Makhov, A. M.; Epperly, M.; Lu, J. Q.; Grab, S.; Zhang, P. J.; Rohan, L.; Xie, X.-Q.; Wipf, P.; Greenberger, J.; Li, S. Nanoassembly of surfactants with interfacial drug-interactive motifs as tailor-designed drug carriers. *Mol. Pharmaceutics* **2013**, *10*, 187−198.
(51) Zhang, P.; Lu, J. Q.; Huang, Y. X.; Zhao, W. C.; Zhang, Y. F.; Zhang, X. L.; Li, J.; Venkataramanan, R.; Gao, X.; Li, S. Design and evaluation of a PEGylated lipopeptide equipped with drug-interactive motifs as an improved drug carrier. *AAPS J.* **2014**, *16*, 114−124.
(52) Han, X. X.; Chen, D.; Sun, J.; Zhou, J. S.; Li, D.; Gong, F. R.; Shen, Y. L. A novel cabazitaxel-loaded polymeric micelle system with superior *in vitro* stability and long blood circulation time. *J. Biomater. Sci., Polym. Ed.* **2016**, *27*, 626−642.
(53) Kim, S. H.; Han, Y.; Kim, Y. H.; Hong, S. I. Multifunctional initiation of lactide polymerization by stannous octoate/pentaerythritol. *Makromol. Chem.* **1992**, *193*, 1623−1631.
(54) Schwach, G.; Coudane, J.; Engel, R.; Vert, M. More about the polymerization of lactides in the presence of stannous octoate. *J. Polym. Sci., Part A: Polym. Chem.* **1997**, *35*, 3431−3440.
(55) Kim, M. S.; Seo, K. S.; Khang, G.; Lee, H. B. Ring-opening polymerization of ε-caprolactone by poly(ethylene glycol) by an activated monomer mechanism. *Macromol. Rapid Commun.* **2005**, *26*, 643−648.
(56) Fan, Y. J.; Chen, G. P.; Tanaka, J.; Tateishi, T. L−Phe end-capped poly(L-lactide) as macroinitiator for the synthesis of poly(L-lactide)-*b*-poly(L-lysine) block copolymer. *Biomacromolecules* **2005**, *6*, 3051−3056.
(57) Dash, T. K.; Konkimalla, V. B. Poly-ε-caprolactone based formulations for drug delivery and tissue engineering: A review. *J. Controlled Release* **2012**, *158*, 15−33.
(58) Li, L.; Aggarwal, B. B.; Shishodia, S.; Abbruzzese, J.; Kurzrock, R. Nuclear factor-κB and IκB kinase are constitutively active in human pancreatic cells, and their down-regulation by curcumin (diferuloylmethane) is associated with the suppression of proliferation and the induction of apoptosis. *Cancer* **2004**, *101*, 2351−2362.
(59) Sahoo, S. K.; Ma, W.; Labhasetwar, V. Efficacy of transferrin-conjugated paclitaxel-loaded nanoparticles in a murine model of prostate cancer. *Int. J. Cancer* **2004**, *112*, 335−340.
(60) Zou, P.; Helson, L.; Maitra, A.; Stern, S. T.; McNeil, S. E. Polymeric curcumin nanoparticle pharmacokinetics and metabolism in bile duct cannulated rats. *Mol. Pharmaceutics* **2013**, *10*, 1977−1987.
(61) Kim, M. S.; Hyun, H.; Cho, Y. H.; Seo, K. S.; Jang, W. Y.; Kim, S. K.; Gilson Khang, G.; Lee, H. B. Preparation of methoxy poly(ethyleneglycol)-block-poly(caprolactone) via activated monomer mechanism and examination of micellar characterization. *Polym. Bull.* **2005**, *55*, 149−156.
(62) Chen, H.; Kim, S.; He, W.; Wang, H.; Low, P. S.; Park, K.; Chen, J. X. Fast release of lipophilic agents from circulating PEG-PDLLA micelles revealed by *in vivo* forster resonance energy transfer imaging. *Langmuir* **2008**, *24*, 5213−5217.
(63) Letchford, K.; Burt, H. M. Copolymer micelles and nanospheres with different *in vitro* stability demonstrate similar paclitaxel pharmacokinetics. *Mol. Pharmaceutics* **2012**, *9*, 248−260.
(64) Garcea, G.; Jones, D. J.; Singh, R.; Dennison, A. R.; Farmer, P. B.; Sharma, R. A.; Steward, W. P.; Gescher, A. J.; Berry, D. P. Detection of curcumin and its metabolites in hepatic tissue and portal blood of patients following oral administration. *Br. J. Cancer* **2004**, *90*, 1011−1015.
(65) Schmidt, S.; Gonzalez, D.; Derendorf, H. Significance of protein binding in pharmacokinetics and pharmacodynamics. *J. Pharm. Sci.* **2010**, *99*, 1107−1122.
(66) Song, Z. M.; Feng, R. L.; Sun, M.; Guo, C. Y.; Gao, Y.; Li, L. B.; Zhai, G. X. Curcumin-loaded PLGA-PEG-PLGA triblock copolymeric micelles: preparation, pharmacokinetics and distribution *in vivo*. *J. Colloid Interface Sci.* **2011**, *354*, 116−123.
(67) Hoehle, S. I.; Pfeiffer, E.; Solyom, A. M.; Metzler, M. Metabolism of curcuminoids in tissue slices and subcellular fractions from rat liver. *J. Agric. Food Chem.* **2006**, *54*, 756−764.
(68) Garcia-Alloza, M.; Borrelli, L. A.; Rozkalne, A.; Hyman, B. T.; Bacskai, B. J. Curcumin labels amyloid pathology *in vivo*, disrupts existing plaques, and partially restores distorted neurites in an Alzheimer mouse model. *J. Neurochem.* **2007**, *102*, 1095−1104.

DOI: 10.1021/acs.molpharmaceut.6b01171
Mol. Pharmaceutics 2017, 14, 2585−2594